PHILOSOPHICAL TRANSACTIONS OF THE ROYAL SOCIETY A
MATHEMATICAL, PHYSICAL & ENGINEERING SCIENCES

Geological Faults: Fracture, Creep and Strain

G. C. P. King

Phil. Trans. R. Soc. Lond. A 1978 **288**, 197-212
doi: 10.1098/rsta.1978.0013

Phil. Trans. R. Soc. Lond. A. 288, 197–212 (1978) [197]
Printed in Great Britain

Geological faults: fracture, creep and strain

By G. C. P. King†
Department of Geophysics, Faculty of Science, Ferdowsi University, Mashad, Iran

To extend our understanding of faulting in the Earth's crust it will be necessary to describe the various physical processes of faulting in terms of boundary and initial value problems.

This is not easy to do. Field evidence indicates that faults form geometrically complex systems and time histories depend on the highly nonlinear processes of fracture and friction.

The phenomenon of faulting is reviewed starting with a description of the work of E. M. Anderson who demonstrated that a partial knowledge of the boundary conditions under which faulting could occur allows fault types to be classified.

However, many commonly observed features of fault behaviour are unexplained by Anderson's ideas. These features are described and the various attempts to explain them or reproduce them by modelling are discussed.

Seismic studies are briefly covered and it is noted that seismically determined stress drops can also be interpreted to show that earthquake faults have displacement to length ratios close to 10^{-4}. A similar value has also been found from field observation of intersections of earthquake faults with the ground surface. It is also pointed out that faults observed in the field are always significantly more complex than the simple geometrical models of earthquake sources used in seismology and that this deserves greater study.

1. Introduction

To understand the mechanical behaviour of the Earth's crust we must understand the role of faulting in the processes of crustal deformation. Until the advent of plate tectonics in the 1960s there was a tendency for faulting to be regarded as a secondary phenomenon with ductile deformation being the principal deformation mechanism (Anderson 1951, p. 1). The discovery of major fault systems in the oceans with displacements of more than 1000 km (Mason & Raff 1961; Raff & Mason 1961) showed that at least some faults play a major rôle in the deformation of the crust. A further source of interest in faulting has followed the full realization that earthquakes are due to fault motion and that the only real hope for effective earthquake prediction lies in gaining a proper understanding of fault mechanics. This realization has gained ground steadily since Reid (1910) published his observations of ground deformations associated with the 1906 San Francisco earthquake.

The theory of faulting, such as it is, does not come from global tectonics but from the study of industrial materials. Even seismology, as yet, does no more than provide field measurement of parameters that owe their origin to laboratory sample experiments and it is questionable whether such use is entirely justifiable. Seismology allows active faults to be mapped to depth and is an important adjunct to geological field observation of fault systems. However, the greatest body of literature on faulting consists of geological description and it seems appropriate to review these observations first. This task is hampered by the fact that only a small part of a fault is actually seen in the field and this can lead geologists to interpret their data with the help

† Present address: Department of Geodesy and Geophysics, Cambridge University, Madingley Rise, Madingley Road, Cambridge CB3 0EZ.

of inadequate or incorrect theories. The importance of such prejudices is emphasized by an account given by King–Hubbert (1972, p. 9) of a geologist losing his job for mapping faults (correctly) in a place where theory (incorrectly) was thought to demonstrate they could not occur. I shall, therefore, start with an account of the Anderson fault classification, since, as far as it goes, it is the only correct theory available and it is fairly easy to see the nature of its limitations. It is widely used in geological interpretation.

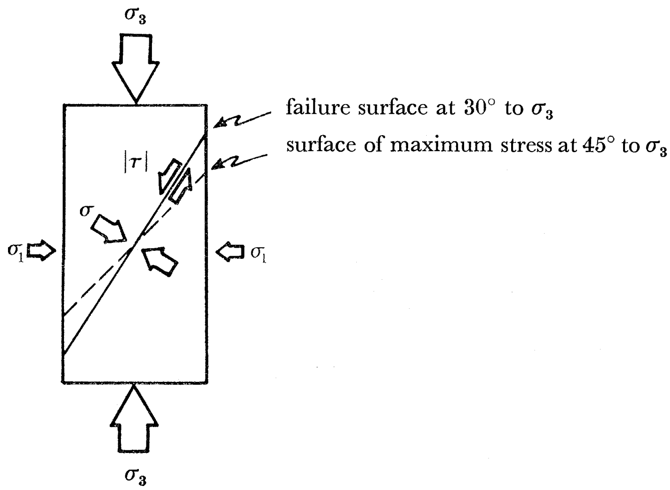

FIGURE 1. The Coulomb failure criterion: $|\tau| = \tau_0+\mu\sigma$, where $|\tau|$ is critical shear stress, τ_0 internal cohesion, μ internal friction, and σ normal stress.

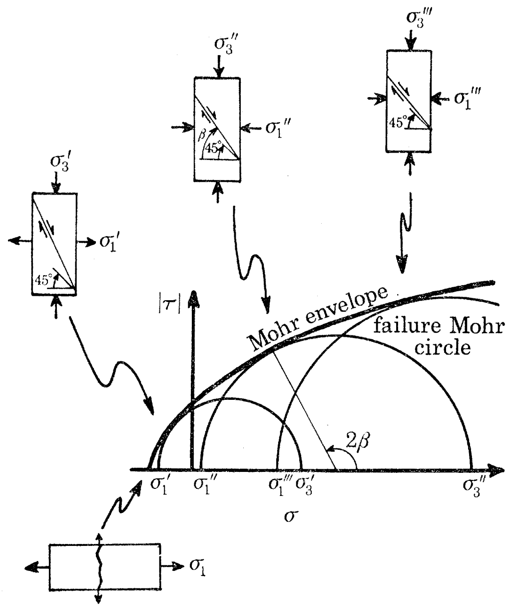

FIGURE 2. The Mohr construction. The cartoons of rock samples show the way in which the angle of failure varies for different parts of the Mohr enveloping curve (envelope).

2. The Anderson criteria

The Anderson criteria are produced by combining empirical results for the failure of rock (derived from the study of laboratory samples) with constraints on stress systems inside the Earth that arise from the existence of the Earth's stress free surface.

Figure 1 shows the Coulomb failure criterion (see, for example, Jaeger & Cook 1969) for a sample under triaxial test conditions. The largest stress is σ_3 and the smallest σ_1. Provided that σ_2 remains such that $\sigma_3 > \sigma_2 > \sigma_1$, then σ_2, the intermediate stress, appears to play no significant part in the failure process. Failure does not occur on the plane of maximum shear but at an angle to it. Coulomb explained this by the introduction of a coefficient of internal friction.

(a)

(b)

(c)

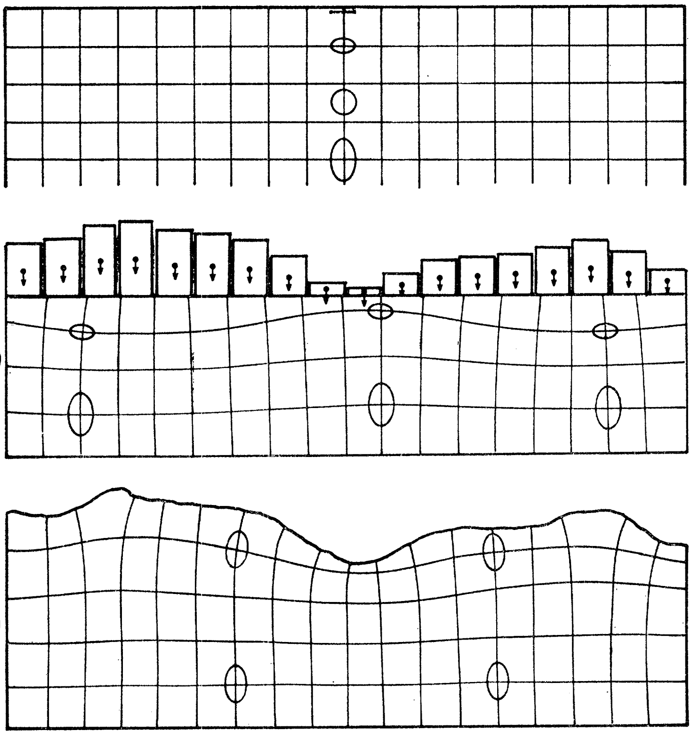

Figure 3. Trajectories of normal stress near the Earth's surface. The conditions near a flat surface are shown in (*a*). These are modified by the affects of the weight of surface topography (*b*), and internal density variations (not shown). External stresses are modified by topography (*c*) and internal rigidity variations (not shown).

The relation between this coefficient in unfractured material and the coefficient between two discrete surfaces is purely notional and it is important to realize that this 'friction' operates even when there are tensile forces acting across the future failure plane. The internal friction does not obey a linear law very well, particularly at low confining pressure, an effect that is conveniently demonstrated with the aid of Mohr's construction (figure 2) (Jaeger & Cook 1969). Mohr's construction is so widely employed to describe failure that the term Mohr–Coulomb failure is often used. Figure 2 shows the angle of failure for idealized rock samples for different stress conditions. For crustal rocks a rough average of 30° to the direction of maximum principle stress was assumed by Anderson.

The only boundary close to a fault about which certain information is known is the Earth's stress free surface. At a stress free surface there are no normal or tangential forces. Thus the surface stress tensor reduces to a flat ellipse in the plane of the surface. One principal axis is vertical and the other two are horizontal (figure 3*a*). Since gravity acts vertically this configuration of principal axes does not change with depth although the magnitudes of the principal stresses change. The Earth's surface is not, in general, flat and this causes the principal stresses to be deflected from the vertical and horizontal. There are two separate topographic effects shown in figures 3(*b*) and (*c*). The first is a deviation of directions due to the spatial

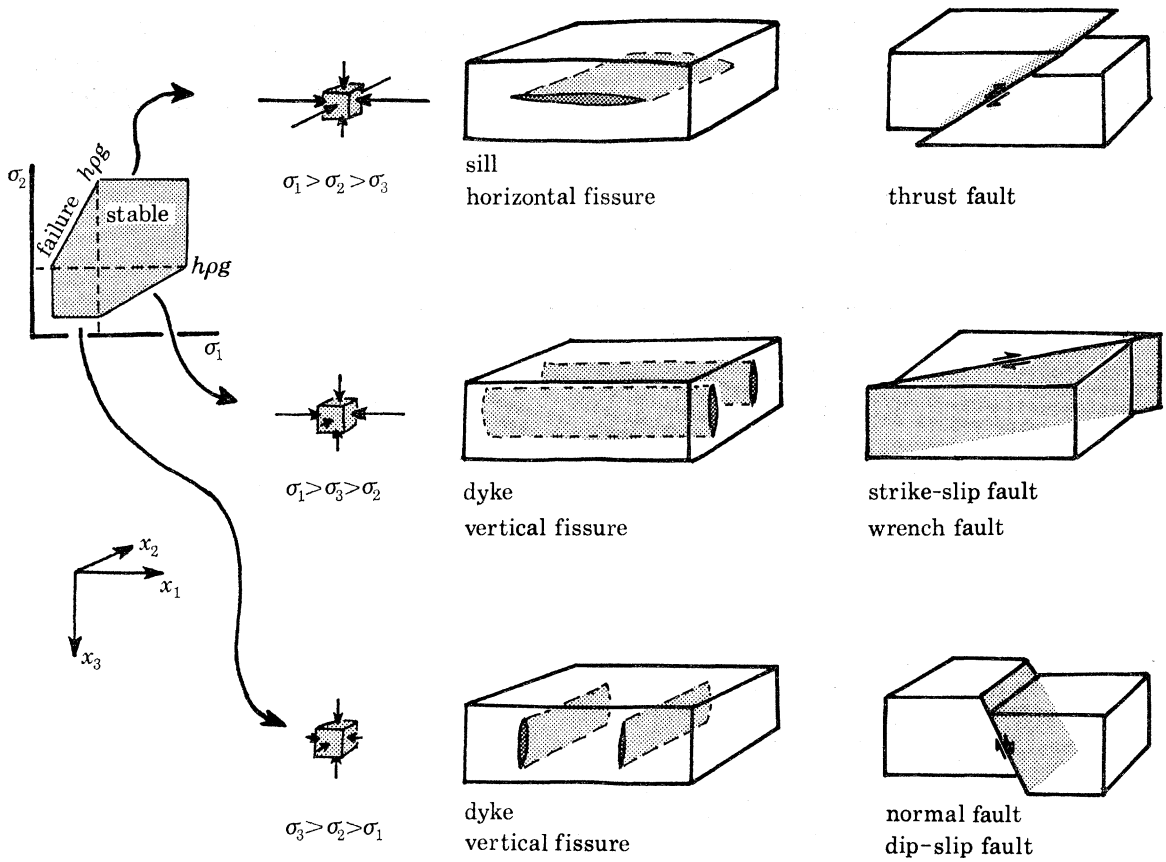

FIGURE 4. The Anderson criteria. The shaded area in the left diagram represents stress conditions under which failure will not occur. The broken lines marked $h\rho g$ indicate the pressure of rock overburden and the diagram is therefore only correct for one depth. The central set of cartoons indicate the tensional structures that can develop if a fluid is present with a pressure intermediate between the greatest and least principal rock stress. At depth, the only fluid with sufficient pressure to produce large fissures is molten rock. Micro-fissures filled with water extend to depths of several kilometres. The cartoons on the right show the faulting that occurs under the same stress conditions in the absence of fluid of sufficient pressure. Conjugate faults are not shown; neither are the fractures that might occur (but are not observed in the field) when two principal stresses have identical values.

variation of the weight of the topography and the second is the effect of the irregular surface on stress systems that act on the region from a distance. This latter effect has been discussed in the tidal literature (for example, Harrison 1976). It is easy to see that the two effects are calculable for any given conditions and to concur with Anderson that, except under conditions of 'Alpine' topography, one principal stress will be nearly vertical and the other two nearly horizontal.

In figure 4 the consequences of combining the stress free surface conditions and the failure criteria are summarized. Three stress conditions are identified, vertical stress being the least, the intermediate, or greatest of the three principal stresses in turn. These give the three classes of faulting shown in the block diagrams on the right. The central diagrams show the fissures that can form under conditions where a fluid is available with a pressure intermediate between the greatest and least principal stresses. Thus horizontal fissures or sills form under the same stress conditions as thrust faults and vertical fissures or dykes under the same conditions as strike-slip or dip-slip faults. The graph on the left shows, for one depth, the stress conditions under which different types of faulting or fissuring occur. It is interesting to notice that the stresses involved in thrust formation are very much greater than those associated with normal faulting and that strike slip faulting can be initiated over a wide range of intermediate stress conditions.

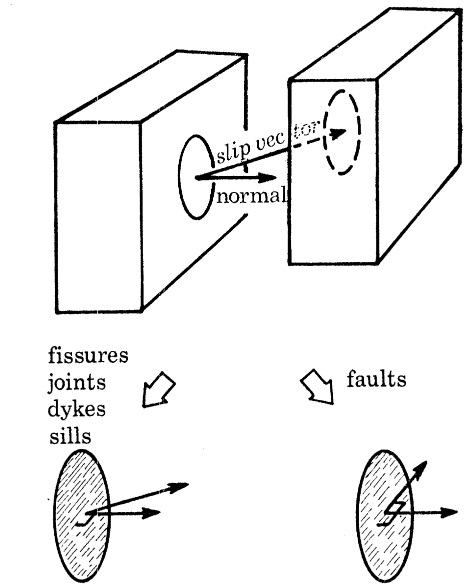

Figure 5. Conservative and non-conservative dislocations. Both conservative and non-conservative rock dislocations occur. Non-conservative dislocations that involve a volume increase are common but those that involve a volume decrease are not common because there are no very effective mechanisms of a macroscopic scale for melting, dissolving (or diffusing) material away from cracks.

The combination of the surface boundary conditions and rock failure criteria places substantial constraints on the type of rock dislocations that should occur. Both conservative and non-conservative dislocations (Nabarro 1967) can occur (cf. figure 5) but the Anderson criteria place severe constriants on the permissable orientations of the fault planes and directions of the slip vector.

3. Deviation of field data from the Anderson criteria

Field observations of faults and dykes broadly fit Anderson's classifications. Dykes are generally vertical or nearly vertical and sills are close to horizontal. Dip-slip faults generally dip at close to 60°, thrust faults at 30° and strike-slip faults have nearly vertical fault planes. The direction of slip appears to be more variable, dip-slip faults may have to up 30 % strike-slip motion and strike-slip faults sometimes have a similar proportion of dip-slip motion. However, field observations of faults define the direction of slip by the direction of scratching (slickensides) on exposed small fault surfaces and a local direction may not be representative of a broader average. Figure 6 shows a histogram of the normals to the nodal planes of fault plane solutions of shallow earthquakes in the Mediterranean (McKenzie 1972) together with a predicted distribution for comparison. There is some similarity between the two distributions but the fit is far from perfect. From a fault plane solution alone it is impossible to distinguish the slip vector from the normal to the fault plane and it is therefore impossible to determine whether the deviation from the Anderson conditions is predominantly due to deviation in the orientation of the fault alone or to the angle of slip.

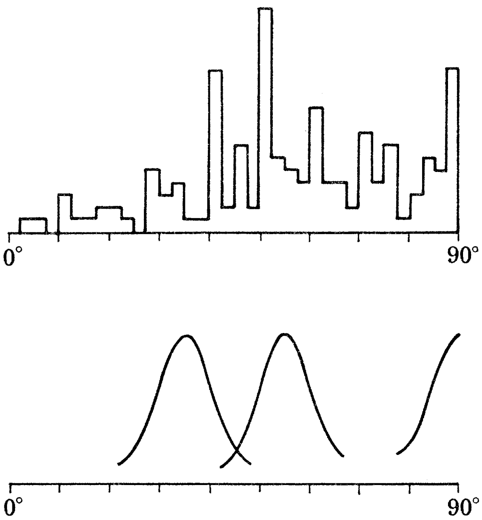

FIGURE 6. The dip of nodal planes of shallow earthquakes. (*a*) For the Mediterranean (from McKenzie 1972) and (*b*) a crude prediction from the Anderson criteria assuming a 5° normal error.

Explanations for deviations from the Anderson criteria fall into three categories:

(*a*) *Inhomogeneity of material properties*. Faults often appear to follow old lines of weakness which either arise from the depositional characters of the rocks or due to pre-existing faults. There is evidence that this is one significant reason for fault planes and slip directions deviating from those predicted (Bott 1958; McKenzie 1969). Very shallow angle thrust faults are common in major mountain belts and are attributed to weakening of sediments due to high water pressure (Hubbert & Rubey 1957; Raleigh & Griggs 1963).

(*b*) *Inhomogeneity of stress pattern*. The stress systems assumed by Anderson are homogeneous and semi-infinite. Topographic effects can cause stress concentrations or these can arise from material properties or as a result of previous fracture history. A stress inhomogeneity which is small in dimensions compared to its depth from the surface is not constrained by the surface boundary conditions and a fracture in it can occur in any direction.

(*c*) *Inhomogeneity of fault motion and Poisson ratio effects*. The Anderson theory assumption of homogeneous stress implies faulting of infinite extent and homogeneous (and strictly speaking infinite amplitude), fault displacement. That faults are not infinite in extent is presumably due to variations of material properties or localization of stresses. A consequence of spatially varying slip amplitudes on faults is Poisson ratio motions perpendicular to the predominant slip direction. Although there are no vertical stresses, vertical strains and hence motion can result from horizontal stresses. The effect is frequently observed on the surface breaks of strike-slip earthquake faults and is known as 'scissoring'. Although the predominant motion of the fault is strike-slip, alternate sides of the fault are up-thrown or down-thrown (Richter 1958).

4. Other field observations

Faulting appears to occur on all scales. Faults range from those with displacements of thousands of kilometres to those with negligible displacements. Perhaps the simplest argument suggesting that faulting occurs on a wide range of scales is the Gutenberg & Richter frequency–magnitude relation which is obeyed both for large and small shocks (Scholtz 1968):

$$\lg N = a + bM, \tag{1}$$

where N is the number of earthquakes per unit time, a and b are constants and M is earthquake magnitude

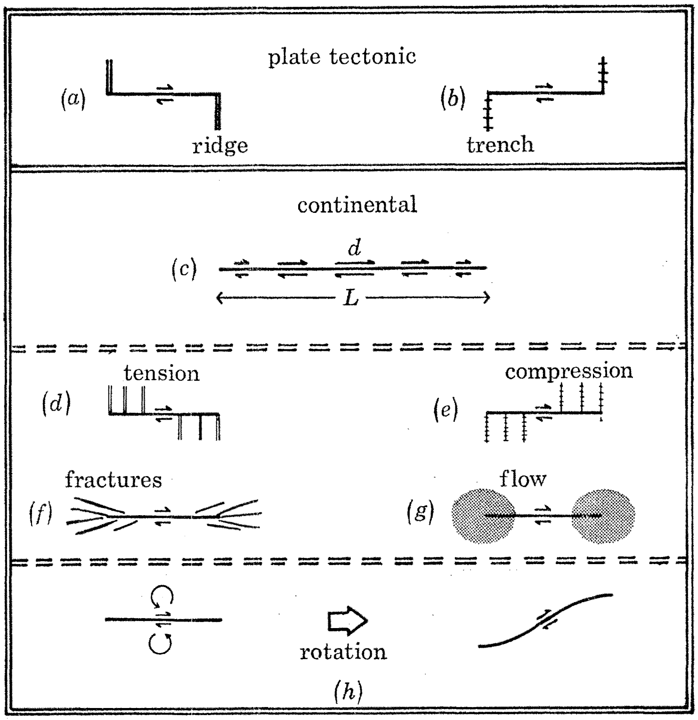

Figure 7. Ways of ending faults; in (c), d = displacement and L = length.

Faults vary in length between many thousands of kilometres to crystalline dimensions. Many faults observed geologically, however, have a surprisingly constant displacement to length ratio in the region of 1:10. This may be compared with the displacement to length ratio, of about $1:10^4$, associated with earthquake motion as observed on the surface breaks of large earthquakes or inferred seismically (Kasahara 1975, in Japanese; see Ohnaka 1976). In both cases the amplitude of the motion decreases progressively towards the ends of the fault in the manner shown in figure 7 (c). This does not apply to the great oceanic transform faults, nor perhaps, to the great thrust and strike-slip faults on continents (Freund 1974; Ranalli 1977). The large-scale geometric behaviour of the transform faults of plate tectonics is well understood; they have constant displacement along their length and terminate at clearly defined features which take up the motion, such as ocean trenches or ridges (Cox 1973). This is shown in figure 7 (*a*, *b*). No such clearly defined features are observed in association with most continental faults. Significant features are not necessary to explain the ending of earthquake faults since the length to displacement ratio is sufficiently small for all the motion to be accommodated elastically. This is not the case for geological faults on continents and figure 7 (*d*–*g*) shows some of the possible ways that displacement may be accommodated. There is no evidence for any one of these mechanisms predominating in general.

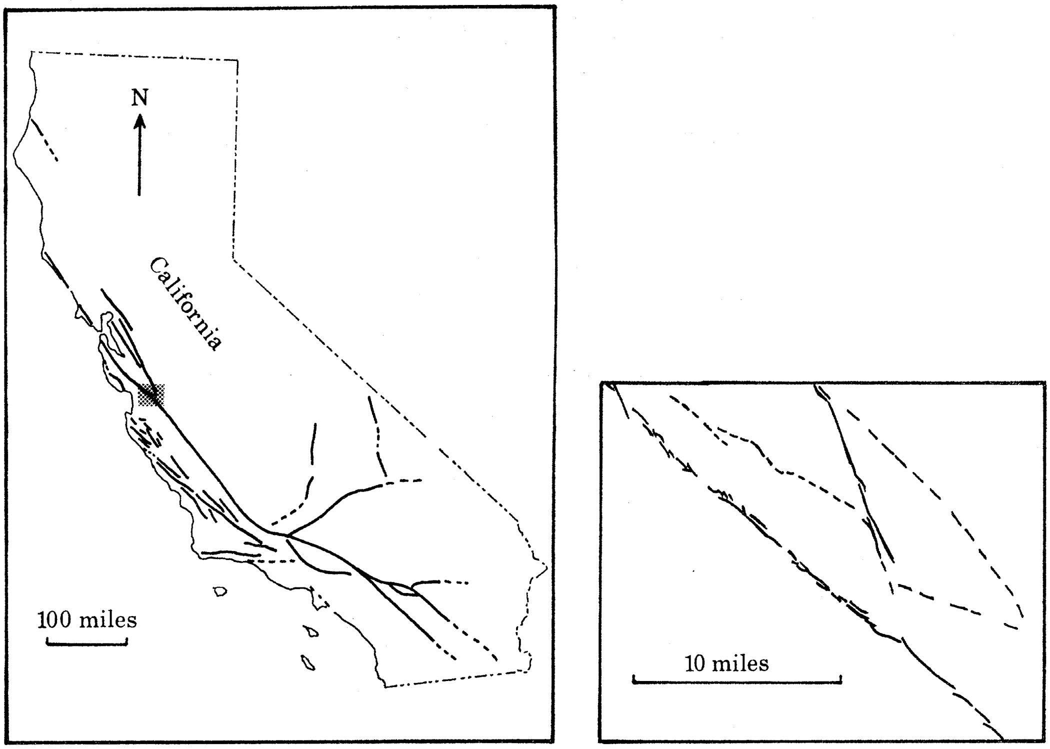

FIGURE 8. The San Andreas fault system (adapted from Moody & Hill 1956, and R. O. Burford, private communication.) The small map is an enlargement of the shaded part of the larger map. The maps are certainly incomplete and many more faults are still to be discovered.

The depth to which faulting usually extends is not clearly known, but is thought to be about 20 km. There are two lines of evidence. The clearest comes from the depth of epicentres. Except in subduction zones (where deep faults do occur), earthquakes are rarely deeper than 15–20 km (Brace & Byerlee 1966). However, since ductile fault processes could take over below this depth, the limit of seismicity does not necessarily delineate the maximum depth of faulting. Geodetic methods have been used to estimate the depth of earthquake faulting but lack sensitivity unless it is assumed that the fault has an abrupt lower boundary (Chinnery 1966).

Another line of evidence comes from the examination of ancient fault zones that have been exposed at the surface by erosion. It is, however, rather difficult to assess the depth at which these zones were active. Depth estimates are based on the pressure and temperature stability of minerals associated with the zone and assumptions about temperature and pressure conditions that existed in the crust at the time of fault formation (Sibson 1977). These cannot be determined accurately. The Anderson theory suggests that faults are simple structures; this is never in practice true. Figure 8 shows the San Andreas fault system on two scales and it can be seen that at both scales it appears as a complex system of fractures. Figure 9 illustrates the general features discernable near a major branch of a *predominantly* strike-slip fault system. Disturbance of the rock is encountered some distance before the fault zone is entered. The rock disturbance may take the form of crushing or shattering of the rock or more gentle warping known as 'drag folding'. The term 'drag folding' arises because it was originally believed that such structures resulted from drag on the fault plane. This cannot be true and these structures must result either from pre-existing weakness near the fault zone or from vertical or horizontal inhomogeneity of fault motion. Inhomogeneous motion causes transient high stress concentrations to occur near the fault zone. This problem has been partly discussed by Garfunkel (1966).

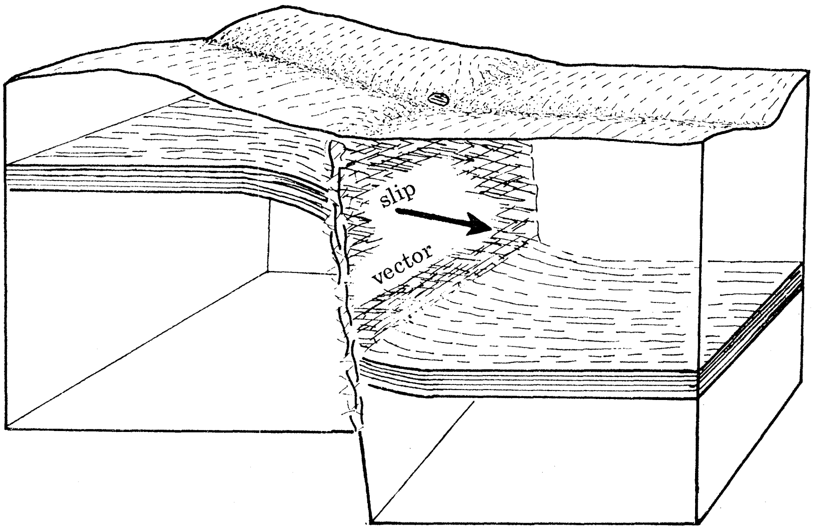

FIGURE 9. Some of the features of a major fault traversed by a river valley.

As the fault zone is approached more closely, the disturbance becomes more intense until a zone is reached where the rocks have suffered so much cataclastic damage that they are no longer obviously similar to the rocks surrounding the fault. This change results partly from mechanical crushing and partly from the chemical changes that the crushing facilitates (Sibson 1977). Within the fault zone are one or more planes across which it is clear that even more intense deformation has been concentrated. On a detailed examination of a fault these are often identified as the 'true' fault plane. However, they do not appear to extend far and are probably not continuous with similar features that can be identified on a traverse across the same fault zone a few hundred metres distant. At the surface, very little of a fault is actually exposed (perhaps a small exposure in a river valley), and faults are generally traced from the slight topographic expression that results from mechanical processes or from selective erosion of different rock types.

5. The problem of scaling

A striking feature of faults is the observation that large fractures appear to be composed of smaller fractures which are, in turn, made up of smaller fractures still. This had been studied by Tchalenko (1970), who demonstrates substantial similarities between fracture patterns on different scales. An example is shown in figure 10. His observation emphasizes what could be

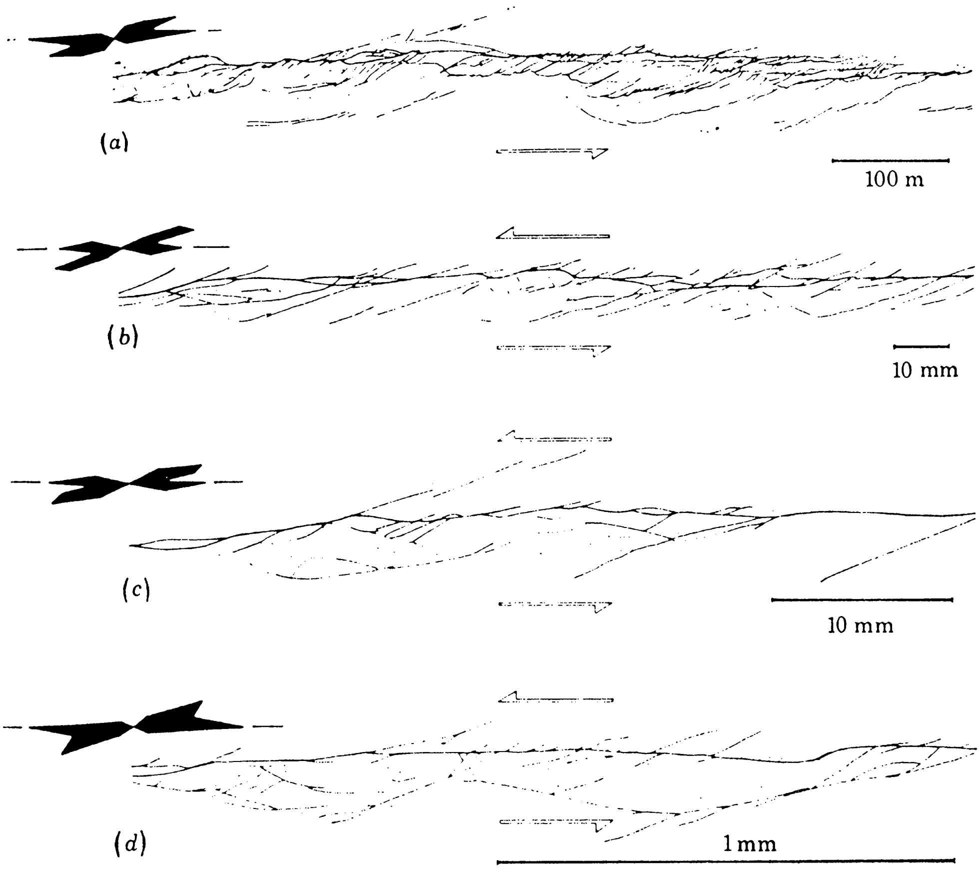

FIGURE 10. Similar fracture patterns on different scales (from Tchalenko 1970). The large-scale diagram (*a*) is taken from a map of surface fractures of the 1968 Dasht-e Bayaz earthquake in Eastern Iran. The other diagrams (*b*–*d*) are from laboratory models.

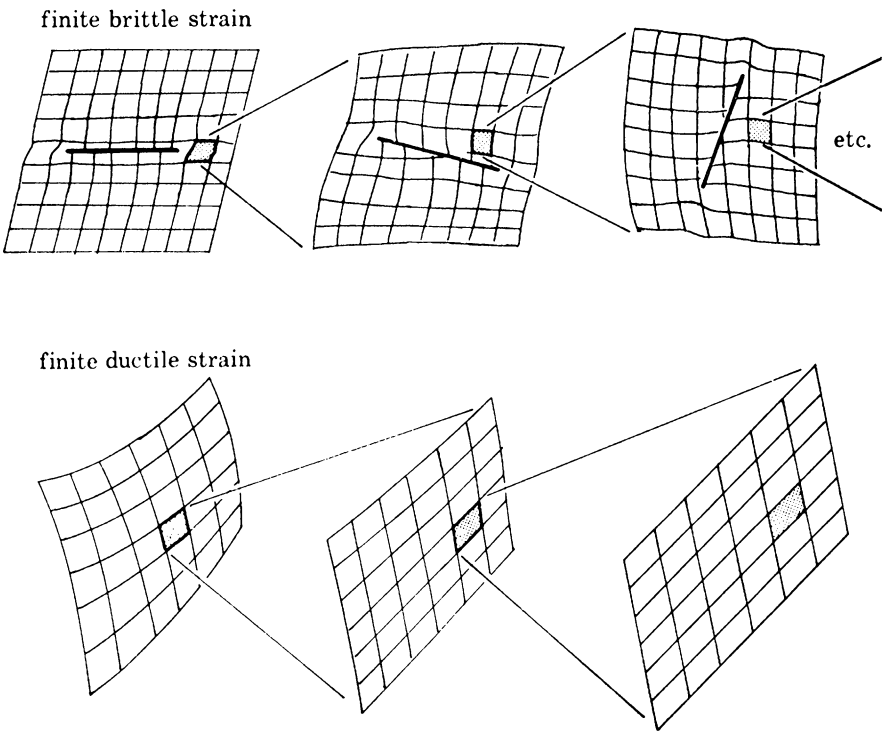

FIGURE 11. Finite brittle and finite ductile strain.

PHILOSOPHICAL TRANSACTIONS OF THE ROYAL SOCIETY A MATHEMATICAL, PHYSICAL & ENGINEERING SCIENCES

described as a 'Russian doll' effect in cataclastic deformation, a behaviour which suggests that the modelling of fault zones cannot be simple. The nature of this difficulty is illustrated by figure 11 which compares the difference between finite strain in a ductile medium (Ramsey 1967) and finite strain in a brittle medium. In the former, a region that is subject to inhomogeneous strain boundary conditions can be divided into smaller regions in which the strain is effectively homogeneous, while in the latter, even large scale homogeneous boundary conditions will result in inhomogeneous strain fields on smaller scales. This emphasizes the fact that Anderson's assumption of stress boundary conditions is not correct except for the instant of initiation of a fracture. It is also clear that strain boundary conditions are not an alternative to stress, and that faulting must take place in an environment intermediate between the two. This has been discussed by anaology to rock press stiffness by Walsh (1971) and Ohnaka (1973). It is also clear that the boundary conditions cannot normally be expected to be homogeneous. This interaction of scales makes fault modelling, either mathematically, or with model materials, rather difficult. I shall briefly outline some of the approaches that have been taken.

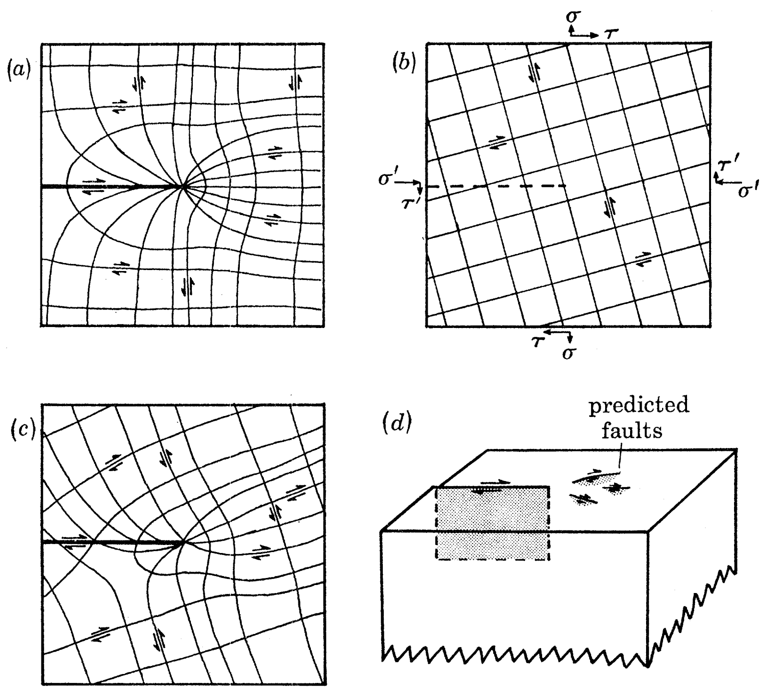

FIGURE 12. Secondary faulting (after Chinnery). Shear stress trajectories of an external field (*b*), summed with the stresses due to a dislocation surface (*a*), give the stress conditions (*c*). The model is shown in (*d*) on approximately the same scale. Some of the predicted secondary faulting is also shown.

6. Further theories of faulting

Chinnery (1966) adapted an idea initiated by Anderson to explain the origin of complex fault structures. The argument depends on the assumption that a fault has for 'some reason' ended leaving a high stress concentration and for 'some reason' the next fracture does not simply extend the main fault. The conditions are shown in figure 12. Chinnery superposes an external field on the stress field produced by an internal cut representing the fault that has already moved. Assuming that the original plane does not extend, he determines, using Coulomb–

Mohr criteria, where new fractures might initiate. Many of these are not in direct line with the original cut but form at angles to it. His principle justification for his model, in particular for his use of a simple cut with uniform displacement across its faces and for the non-propagation of the original fault, is that his predictions accord with field data. This may be true in some field cases. However, it is questionable whether his theory explains field data better than that of Moody & Hill (1956) whose ideas he correctly shows to be wrong.

Figure 13 (*b*, *c*) shows some experiments carried out with analogue materials designed to explain the same features that Chinnery seeks to model. Arguably they all fit the field observations and there appears to be, as yet, no reason to favour any one model on this basis. The most interesting feature of all the models, surprising in the case of figure 13 (*b*), is that fracture initiates at the surface. (In the case of (*b*), surface fractures appear before the fracture, which starts at the base, reaches the surface.)

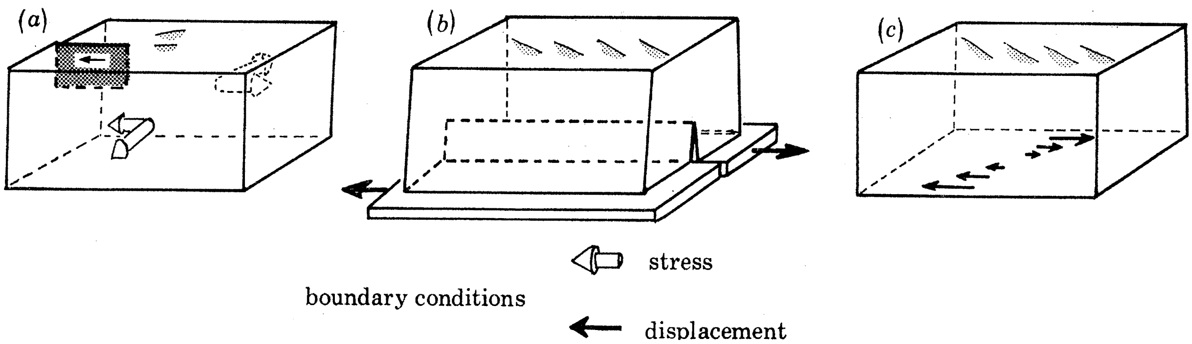

FIGURE 13. Experiments modelling secondary faulting. (*a*) Chinnery's model. The distant boundaries are subject to stress conditions, the internal cut to displacement conditions. (*b*) The Reidel deformation method used by Tchalenko. An analogue material is deformed by the relative displacements of two basal slabs. The other boundaries are made distant. (*c*) Deformation method used by Freund. The lower boundary is constrained to constant shear strain. The lateral boundaries are made distant.

7. Further studies of failure mechanisms

An important modification to Coulomb's internal friction theory of faulting was introduced by Griffith (1924); Jaeger & Cook (1969) who suggested that fracture results from extensional failure due to stress concentrations at the ends of pre-existing flaws in the material (figure 14 (*a*, *c*)). The theory has been quite successful in modelling Mohr envelope shapes at low stresses. However, Bombalakis (1968) has shown that tensional extension of single fissures or simple arrays of fissures (figure 14 *b*) do not lead to failure but to another stable condition. This renders these theories, while empirically satisfactory, physically unsatisfactory. McClintock & Walsh (1962) have modified Griffith's theory by considering the effect of friction across crack surfaces. At high stresses this produces results identical to those of Coulomb but they are no more satisfactory physically.

Since it was appreciated that the mechanical stiffness of the deformation apparatus used to experiment with rock samples has a significant affect on the results, many tests have been carried out over a range of stiffnesses. The two end conditions are constant stress and constant displacement. Under stress conditions any negative gradients in the slope of the stress–strain curve leads to large amounts of energy being 'dumped' into the sample with a consequent catastrophic failure. The same sample, however, subject to displacement conditions can fail progressively, retaining considerable strength after the onset of failure. This led to the discovery that highly fractured rock could support shear stresses approaching that of virgin material (Hobbs 1966; Byerlee 1967; Brace 1968).

Recent interest has centred on the effect of machine stiffness on stick-slip sliding of precut surfaces (Byerlee & Brace 1968; Jaeger & Cook 1971) and how this relates to the conditions experienced by rocks at faults (see §5). Another approach to the study of failure was initiated by Mogi (1962) and taken up by Scholtz (1968). They attached transducers to rock samples under stress to examine acoustic (mainly ultrasonic) emission. Small events begin at stresses considerably less than failure stress and these events concentrate progressively on the plane where failure will occur. Scholtz examined frequency magnitude relations and sequences of small events following more substantial fracture and demonstrated a striking similarity between this microfracturing behaviour and the behaviour of earthquake aftershock sequences.

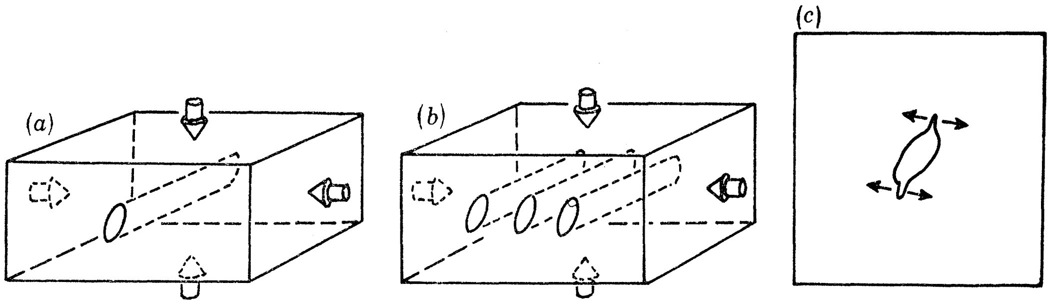

FIGURE 14. Griffith failure. Fracture initiates by extensional failure at crack tips (*c*). These are assumed to be elliptical initially, to facilitate the mathematics. Arrays of cracks (*b*) do not develop fissures that join unless they are so close that their interaction is strong and complex.

8. The seismological view of faulting

At wavelengths large compared to the fault dimension, the spectral displacement amplitude Ω of a seismic wave is given by a function of the type

$$\Omega = Mo\boldsymbol{R}_{\theta\phi}/4\pi\rho R v^3, \tag{2}$$

where $\boldsymbol{R}_{\theta\phi}$ is the radiation pattern of P or S waves, ρ is the near source density, R is a distance function, and v is the P or S velocity. (Keilis-Borok 1959). Burridge & Knopoff (1964) have shown that exactly similar functions result if the source is considered to be a pair of counteracting couples (figure 15*b*) or a dislocation surface (figure 15*a*). In the former case the interpretation of Mo, the seismic moment, is clear; it is the moment of the couples, and has the dimensions of force times distance. In the case of the dislocation interpretation it is physically clearer to use a geometric moment $\boldsymbol{M} = Mo/\mu$. This has the dimensions of length cubed and equation (2) can be rewritten

$$\Omega = \frac{1}{4\pi R}\left(\frac{v_S}{v}\right)^2 \frac{\boldsymbol{M}}{v}\boldsymbol{R}_{\theta\phi}, \tag{3}$$

where v_S is S velocity. The relation between these two moments is similar to that between moment of inertia and moment of cross section in beam theory. The geometric moment is simply $\boldsymbol{M} = S\bar{d}$, where S is the area of the fault plane and $\bar{d}$ the average displacement. From equation (3) it can be seen that seismic amplitudes provide geometric information about the dislocation motion. It is necessary to know the seismic velocity in the source region but it is not necessary to know the shear modulus, or density, separately.

Some of the most useful seismic information in recent years has come from examining the radiation function $\boldsymbol{R}_{\theta\phi}$. This provides the method of fault plane solutions (Honda 1962) which was of such importance in establishing plate tectonics (Cox 1973). The method depends only on establishing the sense of motion of seismic arrivals and is not very sensitive to path effects. The determination of seismic moment, on the other hand, is much more path dependent and the determination and application of appropriate corrections is critical.

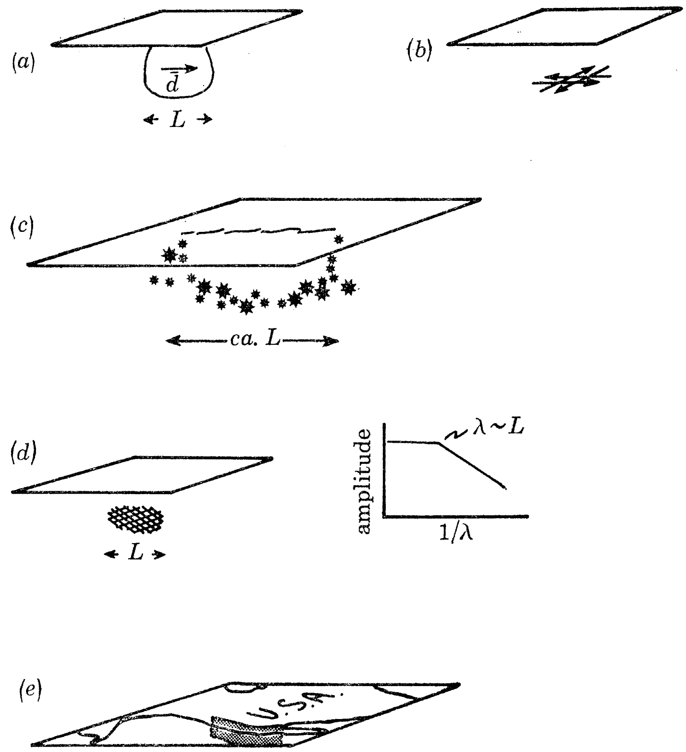

FIGURE 15. Seismic fault parameters: (*a*) dislocation representation of an earthquake source; (*b*) double couple source; (*c*) determination of the fault dimensions from aftershock area or surface fractures; (*d*) determination of fault dimensions from the spectral content of seismograms; (*e*) summing seismic moment along a plate boundary to determine average slip rate.

Seismic moment alone is not a very useful parameter. It is necessary to establish additionally either displacement or fault area. Figure 15 (*c*, *d*) illustrates some of the ways in which this can be done. For large near-surface earthquakes, the length of the surface break is a guide to the fault dimensions. Fault dimensions can also be estimated from the extent of the aftershock sequence although this generally extends over a larger region than the original fault. A method developed by Brune (1970) estimates the dimensions of the fault from the wavelength (and hence frequency) at which equation (2) breaks down because of the effect of finite source size. The spectral character of a seismogram changes at this frequency giving a guide to source dimensions. Either of these methods allows average slip to be determined provided that assumptions about the fault geometry are made. A common assumption is that the fault plane is circular giving $S = \frac{1}{4}\pi L^2$, where L is the fault length. A quantity frequently discussed is stress drop, defined as

$$\Delta\sigma = \mu\bar{d}/L = Mo/L^3.$$

PHILOSOPHICAL TRANSACTIONS OF THE ROYAL SOCIETY A MATHEMATICAL, PHYSICAL & ENGINEERING SCIENCES

This is no more than the ratio of the average displacement divided by the fault length multiplied by a local elastic modulus (and, if the fault geometry is considered carefully, a shape factor close to unity). Average stress drops of 30 bar are not accepted as the mean but stress drops between 10 and 100 bar are common (Kanamori & Anderson 1975). Alternatively, stress drop can be viewed in terms of the displacement: length ratio

$$\bar{d}/L = M/L^3,$$

which gives ratios of around $1:10^{-4}$ (Ohnaka 1973). The moduli assumed near different faults do not vary much so that stress drop and displacement to length ratio are, in practice, a measure of the same thing and perhaps it is easier to visualize the significance of the latter rather than the former. Although it does not seem surprising that stress drop should vary by an order of magnitude, it does seem surprising that displacement to length ratio should be as constant as that.

Seismic moment has an additional use on plate boundaries (figure 15*e*). Over a period of time, all of the seismicity moment along a boundary can be divided by the area of that boundary and the time period. This gives a slip rate that can be compared with the slip rates determined by other methods (see, for example, Davies & Brune 1971; North 1974).

As yet seismology has contributed relatively little to an understanding of failure processes. However, recent studies of the waveform and high frequency spectra of seismic radiation (see, for example, Kanamori & Anderson 1975; Ohanaka 1976) together with greatly increased computing power may produce important results.

9. Conclusion

Aspects of the behaviour of faults and theories of faulting have been reviewed. The Anderson theory of faulting has been shown to have been a great success and an important aid to field geologists, although it can be shown to have limitations both in theory and practice.

Seismologists have demonstrated that earthquakes result from dislocation motion that occurs when a fault is abruptly initiated or an existing fault plane abruptly increases its displacement. At present, a stick-slip process on a uniform plane is assumed. However, there is substantial field evidence that fault geometries are more complex. This may be of importance in developing seismic source models or it may be useful to use seismology to study the apparent complexity of geological faults.

The author would like to thank the staff of the Faculty of Science, Ferdowsi University, for their assistance during the preparation of this paper, to the Natural Environment Research Council of the U.K. and the United States Geological Survey for some support, to Raphael Freund for very valuable discussions and to Paul Davis for critically reading the manuscript.

References (King)

Anderson, E. M. 1951 *The dynamics of faulting*. New York: Hafner. Reprinted 1972.
Bombalakis, E. G. 1968 *Tectonophysics* **6**, 461–473.
Bott, M. P. H. 1958 The mechanics of oblique slip-faulting. *Geol. Mag.* **96**, no. 2.
Brace, W. F. 1968 *Tectonophysics* **6**, 75–87.
Brace, W. F. & Byerlee, J. D. 1966 *Science, N.Y.* **153**, 990–992.
Brace, W. F. & Byerlee, J. D. 1967 *J. geophys. Res.* **72**, 3639–2648.

Brace, W. F. & Byerlee, J. D. 1968 *J. geophys. Res.* **77**, 3690–3697.
Brune, J. N. 1970 *J. geophys. Res.* **75**, 4997–5009.
Burridge, R. & Knopoff, L. 1964 *Bull. seism. Soc. Am.* **54**, 1874–1888.
Byerlee, J. D. 1967 *J. geophys. Res.* **72**, 3639–3648.
Byerlee, J. D. & Brace, W. F. 1968 *J. geophys. Res.* **77**, 3690–3697.
Chinnery, M. A. 1966 *Can. J. Earth Sci.* **3**, 163–190.
Cox, A. 1973 *Plate tectonics and geomagnetic reversals.* San Francisco: Freeman.
Davies, G. & Brune, J. N. 1971 *Nature, phys. Sci.* **229**, 101.
Freund, R. 1974 *Tectonophysics* **21**, 93–134.
Garfunkel, Z. 1966 *Tectonophysics* **3**, 457–473.
Griffith, A. A. 1924 Theory of rupture. *Proc. Inst. Int Congress appl. Mech.*, Delft, 55, 63.
Harrison, J. C. 1976 *J. geophys. Res.* **81**, 319–328.
Hobbs, D. W. 1966 A study of the behaviour of a broken rock under triaxial compression. *Int. J. Rock Mech. & Mining Sci.* **3**, 11–43.
Honda, H. 1962 Earthquake mechanism and seismic waves. *Geophys. Notes, Tokyo* **15**, Supplement.
Hubbert, M. 1972 *Structural geology.* New York: Hafner.
Hubbert, M. K. & Rubey, W. W. 1957 *Trans. Am. Inst. min. Engrs* **210**, 153–158.
Jaeger, J. C. & Cook, N. G. W. 1969 *The fundamentals of rock mechanics.* London: Methuen.
Jaeger, J. C. & Cook, N. G. W. 1971 *Friction in granular materials, Int. Conf. Struct. Solid Mech. Eng. Des. Civ. Eng. Mater.* (Southampton Univ., 1969), p. 22.
Kanamori, H. & Anderson, D. L. 1975 *Bull. seism. Soc. Am.* **65**, 1073–1095.
Keilis-Borok, V. I. 1959 *Annali Geofis.* **12**, 205–214.
Mason, R. G. & Raff, A. D. 1961 *Bull. geol. Soc. Am.* **72**, 1259.
McClintock, F. A. & Walsh, J. 1962 *U.S. National Congress Appl. Mech., Berkeley* 1962.
McKenzie, D. P. 1969 *Bull. seism. Soc. Am.* **59**, 591–601.
McKenzie, D. P. 1972 *Geol. J. R. astr. Soc.* **30**, 109–185.
Mogi, K. 1962 *Bull. Earthq. Res. Inst. Tokyo Univ.* **40**, 125–173.
Moody, J. D. & Hill, M. J. 1956 *Bull. geol. Soc. Am.* **67**, 1207–1246.
Nabarro, F. R. N. 1967 *Theory of crystal dislocations.* Oxford: Clarendon Press.
North, R. G. 1974 *Nature, Lond.* **252**, 560.
Ohnaka, M. 1973 *J. Phys. Earth* **21**, 285–303.
Ohnaka, M. 1976 *Bull. seism. Soc. Am.* **66**, 433–451.
Raff, A. D. & Mason, R. G. 1961 *Bull. geol. Soc. Am.* **72**, 1267.
Raleigh, C. B. & Griggs, D. I. 1963 *Bull. geol. Soc. Am.* **74**, 819–830.
Ramsey, J. G. 1967 *Folding and fracturing of rocks.* New York: McGraw-Hill.
Ranalli, G. 1977 *Tectonophysics* **37**, 71.
Reid, H. F. 1910 *The mechanics of the earthquake: the Californian earthquake of April* 18 1906. Report of the State Investigation Commission, Carnegie Institute of Washington, **2**.
Richter, C. F. 1958 *Elementary seismology.* San Francisco: H. Freeman.
Scholtz, C. H. 1968 *Bull. Earthq. Res. Inst. Tokyo Univ.* **40**, 125–173.
Sibson, R. H. 1977 *J. geol. Soc. Lond.* **133**(3) (in the Press.)
Tchalenko, J. 1970 *Bull. geol. Soc. Am.* **81**, 1625–1640.
Walsh, J. B. 1971 *J. geophys. Res.* **76**, 8597–8598.